Earth **Surface**
Dynamics
Discussions

Timing of exotic, far-travelled boulder emplacement and paleo-outburst flooding in the central Himalaya

Marius L. Huber[1,2], Maarten Lupker[1], Sean F. Gallen[3], Marcus Christl[4], Ananta P. Gajurel[5]

[1]Geological Institute, Department of Earth Sciences, ETH Zurich, Zurich 8092, Switzerland
5 [2]now at: Centre de Recherches Pétrographiques et Géochimiques (CRPG), CNRS, Université de Lorraine, UMR 7358, 54500 Vandoeuvre-lès-Nancy, France
[3]Department of Geosciences, Colorado State University, Fort Collins, Colorado 80523, USA
[4]Laboratory of Ion Beam Physics (LIP), Department of Physics, ETH Zurich, Zurich 8093, Switzerland
[5]Department of Geology, Tribhuvan University, Ghantaghar, Kathmandu, Nepal

10 *Correspondence to*: Marius L. Huber (marius.huber@univ-lorraine.fr)

Abstract. Large boulders, ca. 10 m in diameter or more, commonly linger Himalayan river channels. In many cases, their lithology is only compatible with source areas located >10 km upstream suggesting long transport distances. The mechanisms and timing of "exotic" boulder emplacement are poorly constrained, but their presence hints at processes that are significant 15 for landscape evolution and geohazard assessments in mountainous regions. We surveyed river reaches of the Trishuli and Sunkoshi, two trans-Himalayan rivers in central Nepal to improve understanding of the processes responsible for exotic boulder transport and the timing of emplacement. Boulder size and channel hydraulic geometry were used to constrain paleo-discharges and boulder emplacement ages were determined using cosmogenic nuclide exposure dating. Modelled discharges required for boulder transport, of ca. 10^3 to 10^5 m^3/s, exceed typical monsoonal floods in these river reaches. Exposure ages 20 range between ca. 1.5 and 13.5 kyrs BP with clustering of ages around 4.5 - 5 kyrs BP in both studied valleys. This later period is coeval with a broader weakening of the Indian summer monsoon and glacial retreat after the Early Holocene Climatic Optimum (EHCO), suggesting Glacial Lake Outburst Floods (GLOFs) as a possible cause for boulder transport. We, therefore, propose that these exceptional events are climate-driven, but counter-intuitively occur in the wake of transitions to drier and warmer climates leading to glacier retreat rather than during wetter periods. Furthermore, the old ages and prolonged 25 preservation of these large boulders in or near the active channels shows that these infrequent events have long-lasting consequences on valley bottoms and channel morphology. Overall this study sheds light on the possible coupling between large-infrequent events and bedrock incision patterns in Himalayan rivers with broader implications on landscape evolution.

1 Introduction

Active tectonics, steep topography, dynamic surface processes, and extensive glacier cover expose the Himalaya to a range of 30 catastrophic events that remain relatively rare on observational time scales and hence are poorly understood. Amongst the most striking manifestations of catastrophic events are earthquakes (Avouac, 2003) and resulting widespread landsliding or valley

fills (e.g. Schwanghart et al., 2016; Roback et al., 2018) or lake outburst floods (LOFs) whereby large volumes of impounded water are suddenly released into the fluvial network (Ives et al., 2010; Ruiz-Villanueva et al., 2017). LOF events in the Himalaya received wide-spread attention as the generated discharges may exceed typical precipitation-induced floods by

35   orders of magnitude (e.g. Costa and Schuster 1988; Cenderelli, 2000; O'Conner and Beebee, 2009; Korup and Tweed, 2007; Wohl, 2013; Cook et al., 2018). LOFs represent both a significant hazard (Kattelmann, 2003; Schwanghart et al., 2016) and an active geomorphic agent of landscape evolution (Wohl, 2013; Cook et al., 2018; Turzewski et al., 2019).

LOF generation can be related to the formation of proglacial lakes at higher elevations, as glacier dynamics or frontal moraines

40   trap meltwater that, when rapidly released, can generate glacier lake outburst floods (GLOFs) (Richardson and Reynolds, 2000). LOFs may also be linked to the sudden damming of river channels by large landslides reaching the valley floor. The impounded water is then prone to catastrophic release as landslide lake outburst floods (LLOFs). A recent inventory of modern GLOF occurrences (1988 – 2017) along the entire Himalayan range shows a recurrence of ca. 1.3 significant GLOF events per year (Veh et al., 2019). A modern inventory of LLOFs has not been compiled as systematically, but recent reviews also suggest

45   widespread occurrences along the Himalayan range (Ruiz-Villanueva et al., 2017). Since most of the existing information about LOFs in the Himalaya is derived from observational or historical records, limited insight is available with respect to the maximum magnitudes that can be expected for these events or the evolution of their occurrence frequency through time, being in the past or in response to climatic change.

50   The majority of LOF events originate in sparsely populated areas, but the steep slopes and high connectivity of upstream fluvial networks mean that flood waves can travel significant distances downstream with adverse effects for population and infrastructure (Ziegler et al., 2014; Schwanghart et al., 2016). The catastrophic draining of impounded lakes generally occurs rapidly, evoking spiky hydrographs (Cenderelli, 2000) and leaves little time for early warning, protection or evacuation measures. Better constraining the controls on LOF magnitude and frequency is, therefore, imperative for improved risk

55   assessments in the Himalaya, especially since these risks may evolve due to anthropogenic climate change and increasing land use change (e.g. Korup and Tweed, 2007; Huggel et al., 2012; Stoffel et al., 2014).

LOFs are generally infrequent but have the potential to provoke rapid incision or aggradation in fluvial systems with a long-lasting impact on erosion rates, sediment yields, and landscape morphology (e.g. Davies and Korup, 2010; Worni et al., 2012;

60   Lang et al., 2013). Tectonically active landscapes develop equilibrium and steady-state topography by balancing rock uplift and erosion over long timescales (>1 Myr) (e.g. Willett and Brandon, 2002). On shorter timescales (<10^5 yr), landscape evolution is characterized by phases of erosion and aggradation induced by changes in climatic forcing and the frequency of flood capable of breaching thresholds of bedload entrainment and bedrock detachment (e.g. Bull, 1991; DiBase and Whipple, 2011). LOFs have the potential to move coarse grain-sizes through the fluvial network that would otherwise be immobile

65   during typical floods. These events may hence promote rapid incision in the upper reaches of mountainous catchments where

Earth **Surface**
Dynamics Open Access
Discussions
EGU

typical monsoonal discharges are too low to mobilize large grain sizes that cover channel beds thereby setting the pace of landscape evolution (Cook et al., 2018). The timing, frequency and magnitude of these events as well as their impact on landscape evolution as discontinuous, singular events is however still poorly understood and documented, emphasizing the need to bridge the gap between modern observations and the long-term evolution of landscapes.

70

To better understand catastrophic erosion and mass transport events as well as their potential impact on landscape evolution and related hazard, we focused on the occurrence, provenance, and mechanisms and timing of large boulder emplacement in central Himalayan river valleys. In the studied valleys, numerous large boulders of ca. 10 m in diameter and more, are found in or near the present-day channel beds. The lithology of many of these large boulders differs from those present on the adjacent hillslopes but are the same as geologic units located 10's of kilometres upstream. Their elevation, well below the last glacial maximum ice extent (e.g. Owen and Benn, 2005), excludes glacial transport. The exact transport mechanisms of such exceptionally large grain sizes remain unknown and may be linked to reoccurring catastrophic events such as LOFs. In this contribution, we test this hypothesis using the boulder geometry and channel hydraulic geometry to estimate paleo-discharges required for their mobilization and use cosmogenic nuclide exposure dating to constrain their emplacement age. We discuss our findings in the context of landscape evolution and natural hazards in the Himalaya and point to possible directions for future research.

2 Study area

The central Himalaya of Nepal accommodate ca. 18 mm/yr of the convergence between India and Eurasia (Ader et al., 2012) that translates into high tectonic uplift rates reaching 10 mm/yr (Bilham et al., 1997; Lavé and Avouac, 2001) and a dramatic topographic gradient where elevations rise from about 200 meters above sea level at the range front to >8000 m of elevation across a horizontal distance of ~150 km. Great earthquakes (Mw ≥ 8.0) along the central Himalayan front happen irregularly with estimated reoccurrence intervals of less than 750 to 1000 years (e.g. Bollinger et al., 2014; Sapkota et al., 2013).

A main fault structure present on the central Himalayan mountain front is the Main Central Thrust (MCT), first named by Heim and Gansser (1938) (Figure 1). The MCT marks a distinct change in rock type and separates Lesser Himalayan rocks, which are mostly phyllites, slates, schists, metasandstones, limestones, and dolomites, as well as minor amounts of gneiss (e.g. the "Ulleri gneiss"), from crystalline Higher Himalayan rocks, which includes mostly augen-, ortho-, and para-gneisses (leucogranites and minor quartzites) within the central Himalayan region (e.g. Gansser, 1964; Stöcklin, 1980; Shrestha et al., 1986; Amatya and Jnawali., 1994; Upreti, 1999; Rai, 2001; Dhital, 2015). Lower-grade metamorphic rocks of the Lesser Himalayan show prograde metamorphosis related to MCT thrusting and increasing in metamorphic grade toward the MCT (from greenschist to amphibolite in the vicinity of MCT). The higher Himalayan units have higher metamorphic grades (amphibolite to granulite facies) compared to the overridden Lesser Himalayan rocks (e.g. Pêcher, 1989; Rai, 2001).

100 The Trishuli and Sunkoshi rivers are the targets of this investigation and are located in central Nepal, northwest and northeast of Kathmandu, respectively. They span the Greater Himalayan range from the arid high-elevation Tibetan Plateau to the Himalayan range front and are tributaries of the Narayani and Kosi Rivers, respectively. Both catchments are separated by a main drainage divide in their headwaters and the moderately-sized Melamchi Khola drainage basin at lower elevation (Fig. 1). The Indian summer monsoon, with highly seasonal distributed rainfall, affects both catchments with peak rainfall from June

105 to September (Bookhagen and Burbank, 2010) that is marked by high river discharge and sediment transport (Andermann et al., 2012).

LOF events have been reported for both river-reaches. The Trishuli has been affected by the breach of lake Longda-Cho in Tibet during August 1964 (ICIMOD, 2011), but little is known about the downstream impact of that event. The studied

110 Sunkoshi reach has been affected by repeated LOF events in 1935, 1964, 1981 and 2016 (Shresta et al., 2010; ICIMOD , 2011; Cook et al., 2018) and the last event of 2016 was closely monitored, revealing the impact of the GLOF, originating from the breach of a Tibetan proglacial lake, on the channel bed morphology (Cook et al., 2018). The upstream catchments of both river-reaches are heavily glaciated and a number of potentially hazardous lakes have been identified (Maharjan et al., 2018) so that it is likely that LOF activity extended in the past.

3 Material and methods

3.1 Sampling

Fieldwork took place during two field campaigns in May and October/November of 2016 along the Trishuli and Sunkoshi main trunk river channels. In the field, boulders visibly larger than the surrounding overall bedload sediment grain-sizes, were sampled for surface exposure dating and boulder provenance analysis (Figure 2, Table 1, Supplement, S1). Samples consisted

120 of ca. 1 to 2 kg of fresh rock from the top of the boulders. Fractured or weathered surfaces on boulders were avoided to minimize potential complications associated with post-depositional erosion. Boulders that exhibited clear evidence of post-depositional movement were not sampled. For large boulders that showed "pristine" surfaces and no evidence of post-depositional movement, flat surfaces were sampled in areas that minimized chances for burial by sediment or vegetation (e.g. the top of the boulder) (Figure 2). Rock material was removed using a chisel or a blade saw and the average sample thickness

125 was recorded (S1 and S3). Topographic shielding was measured in the field with a laser range finder, neglecting vegetation.

3.2 Paleo-hydrologic discharge estimation

Paleo-discharges necessary to transport large grain sizes were computed based on boulder sizes and channel hydraulic geometry. Boulder diameter was determined from high-resolution satellite imagery (Google Earth). A succession of imagery

4

Earth **Surface**
Dynamics
Discussions

EGU

of the same object covering several years was used to calculate an arithmetic mean for boulder diameter to minimize error due
130 to imagery distortion (Table 1). Rock density was estimated based on typical densities reported for the sampled lithologies.
Hydraulic geometry measurements included valley cross-sections and slopes, which are needed to calculate flow channel
characteristics during emplacement and were obtained by digitizing 1:25 000 and 1:50 000 scale maps of the Survey
Department of Nepal (S2). These estimates were made using straight river reaches directly upstream of the studied boulders.

135 Three different approaches were adopted to derive peak discharge values from the boulders surveyed in the Trishuli and
Sunkoshi River valleys: i) the empirical approach after Costa (1983), based on a literature compilation describing average flow
velocity that led to transport of large boulders; ii) Clarke (1996)'s force balance approach which computes cross-sectional
averaged velocities based on methods described by Costa (1983) and Bradley and Mears (1980); iii) the approach of Alexander
and Cooker (2016) that allows flow velocities to be estimated from a theoretical force balance equation and taking into account
140 an impulsive force to account for "inherently unsteady" and "non- uniform" flow. All three approaches take advantage of the
incipient motion principle and compute velocities for turbulent, Newtonian fluid flow when a sediment grain of given
intermediate grain diameter initiates motion on the stream's bed. The Gauckler-Manning formula (Gauckler, 1867; Manning,
1891) was then used to estimate peak discharge from the peak flow velocity determined above and the valley cross-sectional
geometry using the numerical optimization scheme of Rosenwinkel et al. (2017). Peak discharges and maximum flood heights
145 were calculated from flow velocities using the average of two valley cross-sections and bed slope for each boulder considered
(S2). Access to Matlab script is detailed in the code availability section below.

3.3 Surface exposure dating

The samples were prepared in the laboratories of the Geological Institute in the Earth Science Department at ETH-Zürich.
Bedrock was crushed and sieved to 250-1000 μm. Quartz was isolated by magnetic separation followed by five to seven
150 sequential leaching steps with H_2SiF_6 and HCl (2/3 – 1/3 by volume). Meteoric beryllium (Be) was removed by three additional
leachings with HF to dissolve ~10% of the sample mass at each step (Lupker et al. 2012). Pure quartz was dissolved after the
addition of ca. 250 μg of ^9Be carrier solution and Be was isolated using sequential ion exchange column chromatography.
Beryllium-10 (^{10}Be) concentrations were measured for each sample at the Laboratory of Ion Beam Physics of ETH Zurich
using the 0.5 MV TANDY AMS facility (Christl et al., 2013). Cosmogenic exposure ages were computed from the blank
155 corrected $^{10}Be/^9Be$ ratios using the online "Cosmic Ray Exposure program" (CREp) calculator (http://crep.crpg.cnrs-nancy.fr,
Martin et al., 2017) using a global production rate 4.08 ± 0.23 at/g/yr, the ERA40 standard atmosphere and a correction for
geomagnetic dipole moment changes. See Supplement (S3) for more detailed information on sample preparation and exposure
age calculation.

4 Results

160 ### 4.1 Field survey and boulder lithology

We surveyed and sampled a total of 16 boulders: ten boulders in the Trishuli River valley, six in the Sunkoshi River valley (Figure 1 and 3; Table 1). Along the Trishuli, the sampled boulders are found in different locations and configurations and have diameters ranging between 8.5 to 18.6 m. Detailed descriptions of the boulders are in S1. In the upstream part of the studied reach, near the village of Betrawati (N27.974; E85.184), boulders are located both in the modern floodplain close to
165 the channel and on top of terrace deposits, ca. 18 m above the present-day channel elevation. Additional boulders ca. 15 km farther downstream, close to the village of Devighat (N27.859; E85.109), are deposited close to the main channel and on top of a tributary fan. Four of ten boulders in the Trishuli valley consist of gneiss, most likely orthogneiss originating from an intrusive protolith. Three gneiss boulders are located downstream of Devighat on a tributary fan and one gneiss boulder is found north of Betrawati (Figure 2, Table 1). In both locations, the surrounding hillslopes are composed of metasedimentary
170 rocks of clearly differing fabric, so it is unlikely that these boulders are locally derived. The other boulders surveyed in the Trishuli valley are bluish or greenish phyllitic schists with a high phyllosilicate content with slightly differing fabrics among samples (Figure 2, Table 1). These boulders have a lithology compatible with the bedrock in the adjacent hillslopes, but also areas farther upstream.

175 Along the Sunkoshi, all the studied and sampled boulders were found within a ca. 3 km from the town of Balephi (N 27.732; E 85.780) and downstream along the Sunkoshi. The six studied boulders have diameters ranging from 4.5 to 29.9 m (Figure 2, Table 1). Only one boulder sampled and surveyed was not exposed in the river channel but was embedded in a terrace deposit just upstream of Balephi Khola's confluence with the Sunkoshi main trunk (Figure 2). The lithology of these Sunkoshi boulders consists of a variety of gneisses (Figure 2, Table 1); some show big porphyric felspar laths deformed to augen structures
180 (NEQ/162 79, 80 and 98). Boulder sample NEQ/162 03, the largest boulder surveyed in this study, has an augen-fabric that looks more homogenous and slightly less deformed than the other samples (Figure 2, Table 1). The lithology of all boulders sampled in the Sunkoshi is different from the schists found in bedrock on the adjacent hillslopes, and they are thus, not locally derived but allochthonous.

4.2 Paleo-hydrologic discharge estimation

185 The average flow velocity values calculated after Costa's (1983) empirical approach are only dependent on the intermediate boulder diameter and range between 7.8 and 16.7 m/s for the surveyed boulders (S2). Flow velocities calculated using a fluid density of 1500 kg/m^3 range between 6.7 and 17.3 m/s using the Clarke (1996) method and between 4.3 and 11.2 m/s using Alexander and Cooker (2016) (S2). Despite minor differences, these three approaches produce similar results (Figure 3). Paleo-discharge derived from these velocities are shown in Figure 3 (and table in S2). Values of Costa (1983), Clarke (1996) and

190 Alexander and Cooker (2016) derived peak discharges range from 3.63×10^3 to 1.97×10^5 m3/s for boulders in the Trishuli and 1.34×10^3 to 1.03×10^5 m^3/s for the boulders in the Sunkoshi.

4.3 Boulder exposure ages

[10]Be cosmogenic exposure ages of boulders in the Trishuli valley have ages ranging between 2.81 and 5.84 ka BP (Figure 4; Table 1) with overall 1σ uncertainties ranging from 0.35 to 0.67 ka and mode of the summed probability density functions
195 around 4.5 kyrs BP. One of the ten boulders, sampled upstream of Betrawati (NEQ/162 59; Figure 4; Table 1; S3) shows a significantly younger exposure age of 1.06 ± 0.29 ka BP, suggesting that the age might suffer from the effects of erosion or more likely burial of the sampled flat top-surface in the terrace deposit during an earlier stage in time and thus does not represent the true emplacement age.

200 The Sunkoshi exposure ages can be assigned to three different age groups (Figure 4): For one boulder, with the smallest intermediate diameter in this study of 4.5 m (NEQ/161 02), the low [10]Be concentration only allows to determine a maximum age of 0.49 ka BP (Figure 2 and 4; Table 1; S3), which could indicate recent emplacement or toppling from an adjacent terrace deposits. The next three older boulders (NEQ/161 01, NEQ/162 98 and NEQ/162 79) show consistent ages within 1σ-uncertainty with 4.98 ± 0.65, 4.97 ± 0.51 and 6.23 ± 0.92 ka BP (Figure 2 and 4; Table 1; S3). Two older boulders are located
205 in the Sunkoshi main channel with exposure ages of 10.96 ± 0.73 ka BP and 13.28 ± 0.96 ka BP (NEQ/162 80 and NEQ/162 03, respectively) (Figure 2 and 4; Table 1; S3).

5 Discussion

5.1 Boulder provenances and travel distances

The schist and phyllite boulder lithologies in the Trishuli valley are associated with the Paleoproterozoic lower Nuwakot group
210 of the Lesser Himalayan sequence and more precisely from the Kuncha formation or the overlying Dangdagaon phyllites that could be found locally in the valley (Stöcklin, 1980; Upreti, 1999). The Trishuli phyllite and schist boulders might, therefore, have travelled only short distances by toppling down from adjacent hillslopes. However, similar to the gneiss boulders, they are in most cases sub-angular to sub-rounded with crescentic abrasion marks suggesting substantial fluvial transport distances (S1). Diagnostic mineralogy and fabric of the other surveyed ortho-gneiss boulders in the Trishuli catchment are not present
215 in the Lesser Himalayan sequence and, therefore, must originate from areas upstream of the MCT (Figure 1). This observation requires minimum transport distances of approximately 22 km to 46 km depending on the present boulder location (Table 1).

A variety of gneiss boulder lithologies are found in the Sunkoshi/Balephi Khola catchment. Ortho-gneiss and augen-gneiss lithologies among boulders around Balephi are of higher metamorphic grade (amphibolite to granulite facies) and must
220 originate upstream to the north across the MCT from Higher Himalayan crystalline rocks present in these areas or from gneiss

to be found just below the MCT in the Lesser Himalayan footwall ("Ulleri type augen-gneiss" for NEQ/162 03, see S1) (Shrestha et al., 1986; Amatya and Jnawali, 1994; Dhital, 2015). This analysis suggests minimum transport distances of ca. 11 to 17 km (Figures 1, Table 1). While the surveyed boulders are mostly located bellow the Sunkoshi/Balephi Khola confluence and could therefore have been transported by both rivers, field observations show an abundance of boulders present in the bed

225 of the Balephi Khola.

As noted above, boulders in both valleys are well below the extent of alpine glaciers in the modern or during the last glacial maximum (e.g. Owen and Benn, 2005; Figures 1 and 2). With glacial transport excluded at these low elevations, this analysis indicates that the mobilization and transport of large grain-sizes occurred in central Himalayan river valleys over long distances

230 (>10 km) through fluvial processes.

5.2 Paleo-discharge estimates

The range of discharge estimates derived in this work is a first-order estimate and carries important assumptions. The sediment concentration of the flow directly influences transport capacity through flow density and flow mechanics (e.g. Pierson and Costa 1987). In hyper-concentrated flows with 40 to 70 wt. % sediment entrained, non-Newtonian, plastic fluid behaviour and

235 laminar flow can arise due to the establishment of shear strength in the fluid material (e.g. Pierson and Costa 1987). However, if the amount of sediment entrainment remains at the lower end of this "hyper-concentrated" range, flow mechanics are still adequately approximated by Newtonian, turbulent flow of a "clear" waterflood (Costa, 1984; Pierson and Costa, 1987; Pierson, 2005; Wang et al., 2009; Hungr et al., 2014) as was assumed here. Other uncertainty arises from the extraction of valley cross-sectional profiles using topographic maps (see S2 for more details). Terrace flats and channel widths are only crudely

240 represented and do not account for past channel morphologies at the time of the floods. Since detailed riverbed morphology is required for the hydraulic discharge calculation, additional uncertainty arises from the resolution of the data used here and the necessity of using the modern channel geometry for these calculations. We hypothesize that these uncertainties are the main reason for the discrepancies between paleo-peak-discharge estimates for boulders from a similar age range that were presumably transported during a single event (Figure 3). First-order discharge estimates for boulder emplacement therefore

245 broadly range from ca. 10^3 to 10^5 m^3/s.

To place our results in the context of previous studies, we compare our discharge to those from the literature and historical records. Cenderelli and Wohl (2001) and Fort et al. (2010) compared seasonal high flow floods (SHFFs) with discharges of recent GLOF and LLOF events and they appeared to be at least one order of magnitude higher than monsoonal precipitation

250 peak discharges in central Himalayan catchments (Kali Gandaki and Mount Everest region). Peak discharges reaching 10^5 m^3/s have been documented or suggested for a few historical events in the Himalaya mainly associated to LLOF such as the Great Indus flood of 1841 (Mason, 1929; Shroder et al., 1991), the great outburst in April 2000 in the Tibetan Yigong Zangbo River (Shang et al., 2003; Delaney and Evans, 2015; Turzewski et al., 2019), and the large LLOFs at Dadu River and Yalong

River in the years 1786 and 1967 in Sichuan province, China (Dai et al., 2005; Runqiu, 2009). These events are, however,
255 rarely observed even though there is sedimentological evidence that large-scale LLOF events happened regularly throughout
the Holocene within the same catchments (e.g. Hewitt et al., 2011; Wasson et al. 2013). To our knowledge, GLOF discharge
estimates of documented events in the Himalaya reach ca. 10^4 m³/s (e.g. Vuichard and Zimmermann, 1987; Hewitt, 1982; Xu,
1988; Yamada and Sharma, 1993; ICIMOD et al., 2011; Cook et al., 2018) with Holocene reconstructed discharge estimates
that exceeded 10^5 m³/s such as for example the Tsangpo River gorge outburst reconstructed by Montgomery et al. (2004).

260

Hydrological stations from the Department of Hydrology and Meteorology, Government of Nepal allow comparison of our
paleo-discharge estimates to measured discharges over the last decades. For the Trishuli reach, station number 447 (N27.97,
E85.18) near the town of Betrawati, is located in between the two studied upstream and downstream boulder fields (Figure 1).
For the Sunkoshi boulders, two stations provide background hydrological information (Figure 1). First, station number 620
265 (N27.80, E85.77) on the Balephi Kola, about 8 km upstream of the most-upstream boulder and 9 km upstream from the
confluence with the Sunkoshi main stem (without any major tributary confluences). Second, station number 610 (N27.79,
E85.9) on the Sunkoshi at Barabise that is located about 14 km upstream of the Balephi Kola and Sunkoshi confluence.
Comparison of the estimated paleo-discharges, which range between ca. 10^3 to 10^5 m³/s, with flow duration curves of the
hydrological stations, shows that flows needed to mobilize the studied boulders generally exceed the largest flows on record
270 (Figure 3 and 5). Discharge records may also include LOF events and, therefore, not only reflect monsoonal precipitation
driven discharge. This finding suggests that typical monsoonal floods are unlikely to have been responsible for boulder
emplacement and that LOFs are the most likely events. The discharge magnitude of these LOFs is on par with historically
recorded LOFs in the Himalayan range.

5.3 Timing of flood events

275 The exposure ages of the Trishuli boulders all cluster around ca. 5 ka BP except boulder samples NEQ/162 44 and NEQ/162
59, which are considered as outliers recording post-depositional erosion or shielding (Figure 4, Table 1). Boulder NEQ/162
59, which shows by far the youngest age, is still buried to a large extent and its top surface is only slightly elevated from the
surrounding ground surface. There is an offset in age (up to 2 kyrs) between exposure ages of boulders currently located on
the fill terrace near the town of Betrawati and boulder ages in the channel or further downstream in the wider valley reach. We
280 interpret the younger ages of these "Trishuli upstream" boulders lying next to the riverbed as the expression of post-
depositional shielding and burial by sediments followed by excavation through river incision in the fill terrace (Figure 2 and
4; Table 1; S1). Boulder NEQ/162 67's lithology varies in fabric from the other schist and phyllites of surveyed boulders in
the Trishuli and could potentially be affected by inheritance (Table 1). Overall the exposure data and interpretation suggest
that boulder transport and emplacement occurred in a single flood event in the Trishuli that happened around 4.9 ± 0.3 ka BP
285 (arithmetic mean with 1σ error of boulder samples NEQ/162 45, 46, 47 and 66; Figure 4; Table 1).

A minimum of two emplacement events are noted in the exposure age data from the Sunkoshi (Figure 4; Table 1). NEQ/161 03 dates back to the late Pleistocene and has the largest maximum diameter determined among surveyed boulders in this study (Figures 2 and 4; Table 1). Boulder NEQ/162 80 yields a younger age and is partly entrained in a fill-terrace deposit (Figure 4; Table 1; S1). We interpret both NEQ/161 03 and NEQ/162 80 as transported during the same event or series of events (within dating uncertainty) that occurred at ~13 ka. This interpretation suggests that NEQ/162 80 was buried by sediments or suffered surface erosion that resulted in the observed ~2 ka age offset (Figure 4; Table 1).

Boulders NEQ/161 01 and NEQ/162 98 show strikingly similar mid-Holocene exposure ages (Figure 4; Table 1). We suppose that these boulders were already exposed or were excavated shortly after emplacement by monsoonal flows from a deposit that once buried the whole tributary junction around the town of Balephi (Figure 4; Table 1; S1). Although the older exposure age of 6.23 ± 0.92 ka BP for boulder NEQ/162 79 is associated with higher uncertainty, it can still be considered synchronous with NEQ/161 01 and NEQ/162 98 within uncertainty. The maximum exposure age of 490 years obtained for NEQ/161 02 (Figures 2 and 4; Table 1), which is the smallest boulder surveyed, suggests movement and toppling by younger smaller LOFs, monsoonal flows, or recent erosion. These data and interpretations suggest that a second phase of valley aggradation and large boulder transport in the Sunkoshi / Balephi Kola occurred at 5.0 ± 0.4 ka BP, based on the arithmetic mean with 1σ error of boulder samples NEQ/161 01 and NEQ/162 98 (Figure 4; Table 1). Importantly, this second flooding event at ~5 ka was not as large as the preceding event at ~13 ka as it did not mobilize boulders > 10 m in diameter (Table 1).

Trishuli boulder ages (without NEQ/162 59) and two ages among the Sunkoshi boulders show a clustering around 5 ka BP across a major drainage divide in the central Himalaya (Figure 1 and 4). At least two older ages in the Sunkoshi indicate flooding during the late Pleistocene (Figure 4); similar ages were not observed in the Trishuli valley (Figure 4). The events that emplaced these large-sized boulders, ca. 10 m in diameter or more, are rare since they represent the remnants of the last largest floods that were not re-mobilized by subsequent floods. The resolution of ^{10}Be exposure ages and uncertainty on the state of dated boulder surfaces does not definitely point toward a single event that affected both catchments. Boulder emplacement could potentially be the result of a series of events that occurred in a short time period of a few hundred years within the range of dating uncertainty (Figure 4). However, the assumption that the boulder emplacements only record a flood of maximum magnitude (see above), the rarity of emplacement, and the absence of obvious stratification in the fill terraces (Figure 2; S1) point toward a single mid-Holocene emplacement event in each valley.

The timing of the Trishuli and Sunkhosi events found in this study is comparable to another large event responsible for the extensive fill terraces found in the central Himalayan Marsyandi river valley about 90 km to the west of the Trishuli valley (Pratt-Sitaula et al., 2004). The authors of that study found large terraces ("Middle terraces") composed of heterolithic conglomerates and boulders with lithologic evidence for transport distances of over 40 km. These fill terraces were interpreted as the result of a single massive earthquake-triggered landslide event that caused a catastrophic debris flow. Recalibrated radiocarbon ages of that infill date back to 4.6 to 5.1 ka BP (Yamanaka, 1982; ages recalculated with OxCal online calibrator,

Earth **Surface**
Dynamics
Discussions
EGU
Open Access

Bronk-Ramsay, 2013). The ages determined for the Trishuli and Sunkhosi boulders are however older compared to the exposure age of another studied large, far-travelled, boulder capping the Pokhara formation, further West in Nepal (ca. 1680 C.E.) (Fort et al., 1987; Schwanghart et al., 2016). The emplacement of this later boulder was linked to a historical 1681 C.E. earthquake even though the magnitude and epicentre of this later event remain poorly constrained (Chaulagain et al., 2018).

325 **5.4 Triggers of Holocene catastrophic LOFs**

Our results demonstrate that high magnitude peak discharge (10^3 to 10^5 m^3/s) by lake outburst events (LOFs) are needed to explain the emplacement of large boulders in the Trishuli and Sunkoshi drainage catchments and that these events were clustered in time at around 5 kyrs in at least two distinct valleys (Figures 3, 4 and 5). To attribute these events to LLOFs or GLOFs requires evaluating our data in light of typical earthquake recurrence times and regional climate variability.
330 Earthquakes and their associated co-seimsic landslides provide a mechanism that could synchronously emplace large landslide dams in main valleys across water divides, exposing downstream reaches to LLOF events. Climate variability, through its modulation of glacier extent and proglacial lake volumes, can also be invoked as a potential trigger of large GLOF events in multiple valleys during a short period of time as observed in our data.

335 The timing of the boulder emplacement in the Trishuli and Sunkoshi/Balephi Kola suggests that these high magnitude flows last occurred ca. 5 kyrs ago. Older, larger boulders in the Sunkoshi/Balephi Kola suggest flows of even higher magnitude affecting trans-Himalayan valleys in the late-Pleistocene. While the dating precision available cannot strictly point towards a synchronous emplacement amongst the studied valleys (and the Marsyangdi, Pratt-Sitaula et al., 2004), major to great earthquakes ($\geq$ Mw 7.0 and 8.0 respectively) periodically rupture large parts of the Main Himalayan Thrust resulting in surface
340 ground shaking over distance > 100s of km along the Himalayan range (e.g. Bilham, 2019). These earthquakes can trigger a large surface response with intense coseismic landsliding as was observed during the 2015 Mw 7.8 Gorkha earthquake (Roback et al., 2018). Although the 2015 earthquake did not result in significant valley blocking due to landsliding that can result in large LLOFs, the total volume of co-seismic landsliding scales with earthquake magnitude (Marc et al., 2016) and hence LLOFs might be more likely following earthquakes with magnitudes larger than Gorkha. Great earthquakes ($\geq$ Mw 8.0) in the
345 Himalaya susceptible to trigger large volumes of landsliding beyond what was observed during Gorkha have estimated recurrence times of 750 to 1000 years (Bollinger et al., 2014; Sapkota et al., 2013). If great earthquakes had a large likelihood to trigger widespread LLOFs (as would be required to explain the emplacement of boulders and valley fills in two to three valleys), we would expect the central Himalayan valleys to be strewn with boulders of younger and possibly more diverse ages owing to the geologically frequent recurrence interval of such events. While earthquake-triggered LLOFs cannot be entirely
350 excluded we do not favour this explanation for the emplacement of the boulders that are the focus of this investigation.

Climate change may be another LOF trigger through its modulation of glacier dynamics and the creation of GLOF-prone proglacial lakes. Multiple terrestrial records for the monsoon-influenced Himalaya and the Indian subcontinent indicate a wet

and strong monsoon phase during the Early Holocene Climatic Optimum (EHCO), followed by a dry phase between 5 ka to 4

355 ka BP. This dry phase is recorded amongst other proxy records, by a compilation of Indian monsoon records (Herzschuh, 2006); the transition to more arid conditions in central India that lead to a vegetation transition towards C_4 grasses as recorded in the Lonar Crater Lake sediments (Sarkar et al., 2015); changes in moisture sources as indicated by a drop in $\delta^{18}O$ of the Guliya ice cap on the Tibetan plateau (Thompson et al., 1997) (Figure 6). In response to the decrease in monsoonal precipitation, a number of preserved glacial landforms in the central Himalaya show a phase of glacial retreat around 5 ka BP

360 (Abramowski et al. 2003; Finkel et al. 2003; Gayer et al. 2006; Schaefer et al. 2008; Pratt-Sitaula et al. 2011; Figure 6). This retreat has not been observed in all studied valleys but glacial moraines dated to around 5 ka are reported in the Langtang valley in the upstream Trishuli catchment and in the Macha Khola, Manaslu massif (^{10}Be ages; Abramowski et al. 2003), in the Khumbu Himal (Everest region) with the Thuklha stage (^{10}Be ages; Finkel et al., 2003), as well as ^3He and ^{10}Be ages derived by Gayer et al. (2006) for moraines in the upper Mailun valley, Trishuli catchment suggesting a regional glacial

365 response to aridification (Figure 6). Although the relation between GLOF frequency and ongoing climate change remains unclear (Harrison et al., 2018; Veh et al., 2019), past large phases of glacier retreat have been suggested to increase GLOF frequency (e.g. Walder and Costa, 1996; Clague and Evans, 2000; Wohl, 2013). Moraine dams form especially if fast glacial retreat follows earlier advances (Korup and Tweed, 2007). The documented phase of glacial retreat at ca. 5 ka BP, therefore, represents a possible triggering mechanism for the emplacement of the studied boulders across river drainage divides as it may

370 have resulted in the more-wide spread occurrence of glacier lakes prone to GLOFs. Climatic forcing of GLOFs is therefore a suitable explanation for the emplacement of far-travelled fills in other valleys in the central Himalaya (e.g. Pratt-Sitaula et al., 2004) and agrees with the provenance of a number of gneiss boulders originating from the glaciated Higher Himalayan crystalline. It should also be noted that abrupt climatic shifts such as the one following the EHCO occurred overall less frequently since the LGM compared to the recurrence time of great Earthquakes.

375

The older exposure ages derived in the Sunkoshi catchment, including the largest boulder surveyed in this study (NEQ/161 03 with 29.9 m intermediate diameter, Figure 2 and 4; Table 1), could be attributed to an LGM or post-LGM glacial retreat that lead to events preserved in the channel till today. If correct, our dataset reflects that long-term climate modulated LOFs can alter Himalayan Valleys on 10^3 to 10^4 yr timescales.

380 **5.5 Implications for erosion and geohazards in the Himalaya**

This study found evidence for high magnitude discharge events in the form of outburst flooding in central Himalayan river valleys. A record of exceptional flooding is preserved not only in the form of large boulders but also in the form of large alluvial fills in Himalayan valleys. As mentioned before (Wohl, 2013; Cook et al., 2018), LOFs may be responsible for channel incision and lateral erosion in the upstream reaches of mountainous rivers but may also lead to aggradation and valley fills in

385 the lower reaches with long-lasting impacts on river morphology. LOFs may, therefore, exert a strong control on the timing and locus of fluvial incision. In this study, we suggest that the largest grain-sizes that can be found in the two studied Himalayan

Earth **Surface**
Dynamics
Discussions

valleys are related to large GLOF events that followed a time of regional glacial retreat after the EHCO and at the close of the Last Glacial Maximum. This interpretation argues for a climatic control on incision rates and sediment export in the Himalaya. Furthermore, it leads to the counter-intuitive notion that the erosional engine might be most efficient during, or at the onset of, drier climatic periods as they represent periods of amplified occurrence of large, bedload mobilizing LOF events. Additionally, the fact that these boulders are preserved in the modern-day channel and adjacent fill deposits suggests that channel incision halted at these locations for periods of time subsequent to extreme channel aggradation. These extreme outburst events could, therefore, be key in regulating the episodic nature of fluvial incision (e.g. Pratt-Sitaula et al., 2004; Dortch et al., 2011) and have a long-lasting effect on sediment fluxes exported downstream. Further work on the frequency and magnitude of these events is required to improve our understanding of their role in long-term channel morphology and incision. This future work should also address the relative importance of these events with respect to other catastrophic events in the Himalaya as we note that GLOFs are not the only mechanism that allow for long distance boulder transport and valley aggradation. This is illustrated by the large Pokhara valley fill deposit and boulder emplacement in central Nepal which was attributed to a series of earthquakes (Schwanghart et al., 2016; Stolle et al., 2017) and had long-term impact on valley morphology and sediment fluxes (Stolle et al., 2019).

In the face of anthropogenic climate change, increasing land use by population growth and ongoing investments into hydropower in central Himalayan valleys, GLOF hazard and risk need to be better quantified (e.g. ICIMOD, 2011; Schwanghart et al., 2016). The recent acceleration of ice loss across the Himalayas (Maurer et al., 2019) has led to an increase in proglacial lake water volumes (Wang et al., 2015; Nie et al., 2017) but, surprisingly, has not so far lead to an observable increase in GLOF frequencies (Veh et al., 2019). How these trends will evolve in the near future remains unknown. In this study, we suggest the occurrence of large GLOF events during the phases of glacier retreat after the LGM and at the mid-Holocene climatic transition. The exact timing of these GLOF events in comparison to the climate forcing remains elusive, but it may foreshadow possible future scenarios with significant threats to downstream populations and infrastructure. It should, however, be noted that the volume of water that can be stored in proglacial lakes in the upper reaches of the Himalayan rivers could be significantly lower than volumes stored in proglacial lakes during glacial retreat from larger glacial extent than present. If correct, expected future GLOFs magnitudes could be lower than during the last deglaciation and the Holocene.

6 Summary and conclusion

We provide field observations of large boulders, ca. 10 m in diameter or more, that show lithologic evidence for travel distances of over 10s of kilometres in two central Himalayan valleys, the Sunkoshi and Trishuli. These boulders are well below the LGM ice extent and therefore require exceptional flows to explain the long travel distances. Using the boulder's estimated masses and an assumption on flow density and regime, we estimated that discharges of 10^3 to 10^5 m^3/s are required to mobilize these grain sizes. Such discharges are, however, higher than typical monsoonal floods as constrained by hydrological data from

nearby locations and therefore suggest that boulder emplacement occurred through high magnitude and catastrophic lake
420   outburst floods.

Cosmogenic nuclide exposure dating ([10]Be) shows emplacement ages of between 4.7 - 5.2 ka BP in the Trishuli valley and
between 4.6 - 5.4 ka BP and 12.2 -14.2 ka BP in the Sunkoshi valley. Our data suggest that the younger events are correlated
across water divides and possibly also with other deposits in the central Himalaya (Marsyandi valley, Pratt-Sitaula et al., 2004).
425   The trigger for these LOF events remains difficult to constrain owing to the limits in dating precision that do not allow to
clearly identify one single event across drainage divide or multiple events occurring within a short amount of time (ca. 1 kyr).
Landslide lake outburst floods following a large seismic event and extensive co-seismic landsliding remains a possible
explanation for boulder transport and emplacement; however, in this case, we argue against this interpretation because the
typical recurrence time for great earthquakes in the Himalaya is on the order of 1 kyrs, relative to the evidence of mid-Holocene
430   and late Pleistocene LOFs in this study. In the case of coseismic LLOF events, we would expect boulder deposits to have
younger and/or more widespread ages. Alternatively, glacier lake outburst floods are also able to generate the required
discharges. Terrestrial climatic records show that the Indian continent and the Himalaya experience significant aridification
trend between 4 to 5 ka BP that follows a period of intense monsoon during the early Holocene climatic optimum. Glacier
reconstructions show evidence for regional glacier retreat during that period as a response to a weaker monsoon. We, therefore,
435   suggest that the observed boulders were most likely mobilized by GLOF events occurring during phases of glacial retreat.

These findings and interpretations have important implications regarding the dynamics of channel incision and erosion rates
in the Himalaya. The role of these exceptional events as geomorphic agents of landscape evolution has recently been
emphasized. We supplement these findings by showing that the studied central Himalayan river channels preserve traces of
440   these large events that occurred 4 to 14 kyrs ago, suggesting a long-lasting impact on sediment dynamics and channel evolution.
Furthermore, even though there is currently no evidence for an increase in GLOF frequencies as a response to anthropogenic
climate change in the Himalayas, the type of evidence put forward in this work suggests that major phases of glacier retreat
may be associated with GLOFs that may, if not be more frequent, at least be of large magnitude.

7 Acknowledgments

8 Code availability

All paleo-hydrologic discharge calculations can be repeated using a user-friendly Matlab script accessible via the URL
450   https://gitlab.com/mlh300/bouldersforpaleohydrology/ and detailed in the affiliated explanatory file.

References

Abramowski, U., Glaser, B., Kharki, K., Kubik, P.W., Zech, W., 2003. Late Pleistocene and holocene paleoglaciations of the Nepal Himalaya: 10Be surface exposure dating. With 5 figures. Zeitschrift fur Gletscherkunde und Glazialgeologie 39, 183–196.

Ader, T., Avouac, J.-P., Liu-Zeng, J., Lyon-Caen, H., Bollinger, L., Galetzka, J., Genrich, J., Thomas, M., Chanard, K., Sapkota, S.N., 2012. Convergence rate across the Nepal Himalaya and interseismic coupling on the Main Himalayan Thrust: Implications for seismic hazard. J. Geophys. Res. 117.

Alexander, J., Cooker, M.J., 2016. Moving boulders in flash floods and estimating flow conditions using boulders in ancient deposits. Sedimentology 63, 1582–1595.

Andermann, C., Crave, A., Gloaguen, R., Davy, P., Bonnet, S., 2012. Connecting source and transport: Suspended sediments in the Nepal Himalayas. Earth and Planetary Science Letters 351, 158–170.

Avouac, J.-P., 2003. Mountain building, erosion, and the seismic cycle in the Nepal Himalaya. Advances in geophysics 46, 1–80.

Bilham, R., 2019. Himalayan earthquakes: a review of historical seismicity and early 21st century slip potential. Geological Society, London, Special Publications 483, SP483. 16.

Bilham, R., Larson, K., Freymueller, J., 1997. GPS measurements of present-day convergence across the Nepal Himalaya. Nature Publishing Group 386, 61.

Bollinger, L., Sapkota, S.N., Tapponnier, P., Klinger, Y., Rizza, M., Van Der Woerd, J., Tiwari, D.R., Pandey, R., Bitri, A., Bes de Berc, S., 2014a. Estimating the return times of great Himalayan earthquakes in eastern Nepal: Evidence from the Patu and Bardibas strands of the Main Frontal Thrust. J. Geophys. Res. Solid Earth 119, 7123–7163.

Bollinger, L., Sapkota, S.N., Tapponnier, P., Klinger, Y., Rizza, M., Van Der Woerd, J., Tiwari, D.R., Pandey, R., Bitri, A., Bes de Berc, S., 2014b. Estimating the return times of great Himalayan earthquakes in eastern Nepal: Evidence from the Patu and Bardibas strands of the Main Frontal Thrust. J. Geophys. Res. Solid Earth 119, 7123–7163.

Bookhagen, B., Burbank, D.W., 2010. Toward a complete Himalayan hydrological budget: Spatiotemporal distribution of snowmelt and rainfall and their impact on river discharge. J. Geophys. Res. Oceans 115.

Bradley, W.C., Mears, A.I., 1980. Calculations of flows needed to transport coarse fraction of Boulder Creek alluvium at Boulder, Colorado. Geological Society of America Bulletin 91, 1057–1090.

Bronk-Ramsay, C., 2013. OxCal software version 4.3.

Bull, W.B., 1991. Geomorphic responses to climatic change. New York, NY (United States); Oxford University Press; None, Medium: X; Size: Pages: (326 p) pp.

Cenderelli, D.A., 2000. Floods from natural and artificial dam failures. Inland Flood Hazards: human, riparian and aquatic communities 73–103.

Earth Surface
Dynamics
Discussions

Cenderelli, D.A., Wohl, E.E., 2001. Peak discharge estimates of glacial-lake outburst floods and "normal" climatic floods in
485   the Mount Everest region, Nepal. Geomorphology 40, 57–90.

Chaulagain, H., Gautam, D., Rodrigues, H., 2017. Revisiting Major Historical Earthquakes in Nepal: Overview of 1833, 1934,
1980, 1988, 2011, and 2015 Seismic Events, Impacts and Insights of the Gorkha Earthquake. Elsevier Inc.
doi:10.1016/B978-0-12-812808-4.00001-8

Christl, M., Vockenhuber, C., Kubik, P.W., Wacker, L., Lachner, J., Alfimov, V., Synal, H.A., 2013. The ETH Zurich AMS
490   facilities: Performance parameters and reference materials. Nuclear Inst. and Methods in Physics Research, B 294, 29–
38.

Clague, J.J., Evans, S.G., 2000. A review of catastrophic drainage of moraine-dammed lakes in British Columbia. Quaternary
Science Reviews 19, 1763–1783.

Clarke, A.O., 1996. Estimating probable maximum floods in the Upper Santa Ana Basin, Southern California, from stream
495   boulder size. Environmental & Engineering Geoscience 2, 165–182.

Cook, K.L., Andermann, C., Gimbert, F., Adhikari, B.R., Hovius, N., 2018. Glacial lake outburst floods as drivers of fluvial
erosion in the Himalaya. Science 362, 53–57.

Coppus, R., Imeson, A.C., 2002. Extreme events controlling erosion and sediment transport in a semi-arid sub-Andean valley.
Earth Surf. Process. Landforms 27, 1365–1375.

500   Costa, J.E., 1984. Physical geomorphology of debris flows, in: Developments and Applications of Geomorphology. Springer,
pp. 268–317.

Costa, J.E., 1983. Paleohydraulic reconstruction of flash-flood peaks from boulder deposits in the Colorado Front Range.
Geological Society of America Bulletin 94, 986–1004.

Costa, J.E., Schuster, R.L., 1988. The formation and failure of natural dams. Bulletin 100, 1054–1068.

505   Dai, F.C., Lee, C.F., Deng, J.H., Tham, L.G., 2005. The 1786 earthquake-triggered landslide dam and subsequent dam-break
flood on the Dadu River, southwestern China. Geomorphology 65, 205–221.

Davies, T.R., Korup, O., 2010. Sediment cascades in active landscapes. Sediment Cascades: An Integrated Approach. John
Wiley and Sons, Chichester 89–115.

Delaney, K.B., Evans, S.G., 2015. The 2000 Yigong landslide (Tibetan Plateau), rockslide-dammed lake and outburst flood:
510   review, remote sensing analysis, and process modelling. Geomorphology 246, 377–393.

Dhital, M.R., 2015. Geology of the Nepal Himalaya: regional perspective of the classic collided orogen. Springer.

DiBiase, R.A., Whipple, K.X., 2011. The influence of erosion thresholds and runoff variability on the relationships among
topography, climate, and erosion rate. J. Geophys. Res. 116.

Dortch, J.M., Owen, L.A., Caffee, M.W., Kamp, U., 2011. Catastrophic partial drainage of Pangong Tso, northern India and
515   Tibet. Geomorphology 125, 109–121.

Finkel, R.C., Owen, L.A., Barnard, P.L., Caffee, M.W., 2003. Beryllium-10 dating of Mount Everest moraines indicates a
strong monsoon influence and glacial synchroneity throughout the Himalaya. Geology 31, 561–564.

Fort, M.: Sporadic morphogenesis in a continental subduction setting, Zeitschrift für Geomorphologie N.F., Suppl., 63, 9–36, 1987.

520 Fort, M., Cossart, E., Arnaud-Fassetta, G., 2010. Hillslope-channel coupling in the Nepal Himalayas and threat to man-made structures: The middle Kali Gandaki valley. Geomorphology 124, 178–199.

Gansser, A., 1964. Geology of the Himalayas, Regional geology series. London : Wiley.

Gauckler, P., 1867. Etudes Théoriques et Pratiques sur l'Ecoulement et le Mouvement des Eaux. Gauthier-Villars.

Gayer, E., Lavé, J., Pik, R., France-Lanord, C., 2006. Monsoonal forcing of Holocene glacier fluctuations in Ganesh Himal
525 (Central Nepal) constrained by cosmogenic 3He exposure ages of garnets. Earth and Planetary Science Letters 252, 275– 288.

Harrison, S., Kargel, J.S., Huggel, C., Reynolds, J., Shugar, D.H., Betts, R.A., Glasser, N., Haritashya, U.K., Klimeš, J., Reinhardt, L., 2018. Climate change and the global pattern of moraine-dammed glacial lake outburst floods. The Cryosphere 12.

530 Heim, A., Gansser, A., 1938. Thron der Götter: Erlebnisse der ersten Schweizerischen Himalaya-Expedition. Morgarten-Verlag, Zürich.

Herzschuh, U., 2006. Palaeo-moisture evolution in monsoonal Central Asia during the last 50,000 years. Quaternary Science Reviews 25, 163–178.

Hewitt, K., 1982. Natural dams and outburst floods of the Karakoram Himalaya. IAHS 138, 259–269.

535 Hewitt, K., Gosse, J., Clague, J.J., 2011. Rock avalanches and the pace of late Quaternary development of river valleys in the Karakoram Himalaya. Bulletin 123, 1836–1850.

Huggel, C., Clague, J.J., Korup, O., 2012. Is climate change responsible for changing landslide activity in high mountains? Earth Surf. Process. Landforms 37, 77–91.

Hungr, O., Leroueil, S., Picarelli, L., 2014. The Varnes classification of landslide types, an update. Landslides 11, 167–194.

540 ICIMOD, 2011. Glacial lakes and glacial lake outburst floods in Nepal. International Centre for Integrated Mountain Development.

Ives, J.D., Shrestha, R.B., Mool, P.K., 2010. Formation of glacial lakes in the Hindu Kush-Himalayas and GLOF risk assessment. ICIMOD Kathmandu.

Kattelmann, R., 2003. Glacial lake outburst floods in the Nepal Himalaya: a manageable hazard? Nat Hazards 28, 145–154.

545 Korup, O., Tweed, F., 2007. Ice, moraine, and landslide dams in mountainous terrain. Quaternary Science Reviews 26, 3406– 3422.

Lang, K.A., Huntington, K.W., Montgomery, D.R., 2013. Erosion of the Tsangpo Gorge by megafloods, eastern Himalaya. Geology 41, 1003–1006.

Lavé, J., Avouac, J.P., 2001. Fluvial incision and tectonic uplift across the Himalayas of central Nepal. J. Geophys. Res. 106,
550 26561–26591.

Lupker, M., Blard, P.-H., Lavé, J., France-Lanord, C., Leanni, L., Puchol, N., Charreau, J., Bourlès, D., 2012. 10Be-derived Himalayan denudation rates and sediment budgets in the Ganga basin. Earth and Planetary Science Letters 333-334, 146–156. doi:10.1016/j.epsl.2012.04.020

Maharjan, S.B., Mool, P.K., Lizong, W., Xiao, G., Shrestha, F., Shrestha, R.B., Khanal, N.R., Bajracharya, S.R., Joshi, S., Shai, S., Baral, P., 2018. The Status of Glacial Lakes in the Hindu Kush Himalaya - ICIMOD Research Report 2018/1.

Manning, R., 1891. On the flow of water in open channels and pipes, Transactions of the Institution of Civil Engineers of Ireland.

Marc, O., Hovius, N., Meunier, P., 2016. The mass balance of earthquakes and earthquake sequences. Geophys. Res. Lett. 43, 3708–3716.

Martin, L., Blard, P.H., Balco, G., Lavé, J., Delunel, R., LIFTON, N., Laurent, V., 2017. The CREp program and the ICE-D production rate calibration database: A fully parameterizable and updated online tool to compute cosmic-ray exposure ages. Quaternary Geochronology 38, 25–49.

Mason, K., 1929. Indus floods and Shyok glaciers. Himalayan Journal 1, 10–29.

Maurer, J.M., Schaefer, J.M., Rupper, S., Corley, A., 2019. Acceleration of ice loss across the Himalayas over the past 40 years. Science Advances 5, eaav7266.

Montgomery, D.R., Hallet, B., Yuping, L., Finnegan, N., Anders, A., Gillespie, A., Greenberg, H.M., 2004. Evidence for Holocene megafloods down the Tsangpo River gorge, southeastern Tibet. Quaternary Research 62, 201–207.

Nie, Y., Sheng, Y., Liu, Q., Liu, L., Liu, S., Zhang, Y., Song, C., 2017. A regional-scale assessment of Himalayan glacial lake changes using satellite observations from 1990 to 2015. Remote Sensing of Environment 189, 1–13.

O'Connor, J.E., Beebee, R.A., 2009. Floods from natural rock-material dams. Megaflooding on Earth and Mars 128–163.

Owen, L.A., Benn, D.I., 2005. Equilibrium-line altitudes of the Last Glacial Maximum for the Himalaya and Tibet: an assessment and evaluation of results. Quaternary International 138, 55–78.

Pêcher, A., 1989. The metamorphism in the central Himalaya. Journal of Metamorphic Geology 7, 31–41.

Pierson, T.C., 2005. Hyperconcentrated flow—transitional process between water flow and debris flow, in: Debris-Flow Hazards and Related Phenomena. Springer, pp. 159–202.

Pierson, T.C., Costa, J.E., 1987. A rheologic classification of subaerial sediment-water flows. Reviews in engineering geology 7, 1–12.

Pratt-Sitaula, B., Burbank, D.W., Heimsath, A., Ojha, T., 2004. Landscape disequilibrium on 1000–10,000 year scales Marsyandi River, Nepal, central Himalaya. Geomorphology 58, 223–241.

Pratt-Sitaula, B., Burbank, D.W., Heimsath, A.M., Humphrey, N.F., Oskin, M., Putkonen, J., 2011. Topographic control of asynchronous glacial advances: A case study from Annapurna, Nepal. Geophys. Res. Lett. 38.

Rai, S.M., 2001. Geology, geochemistry, and radiochronology of the Kathmandu and Gosainkund crystalline nappes, central Nepal Himalaya. Journal of Nepal Geological Society 25, 135–155.
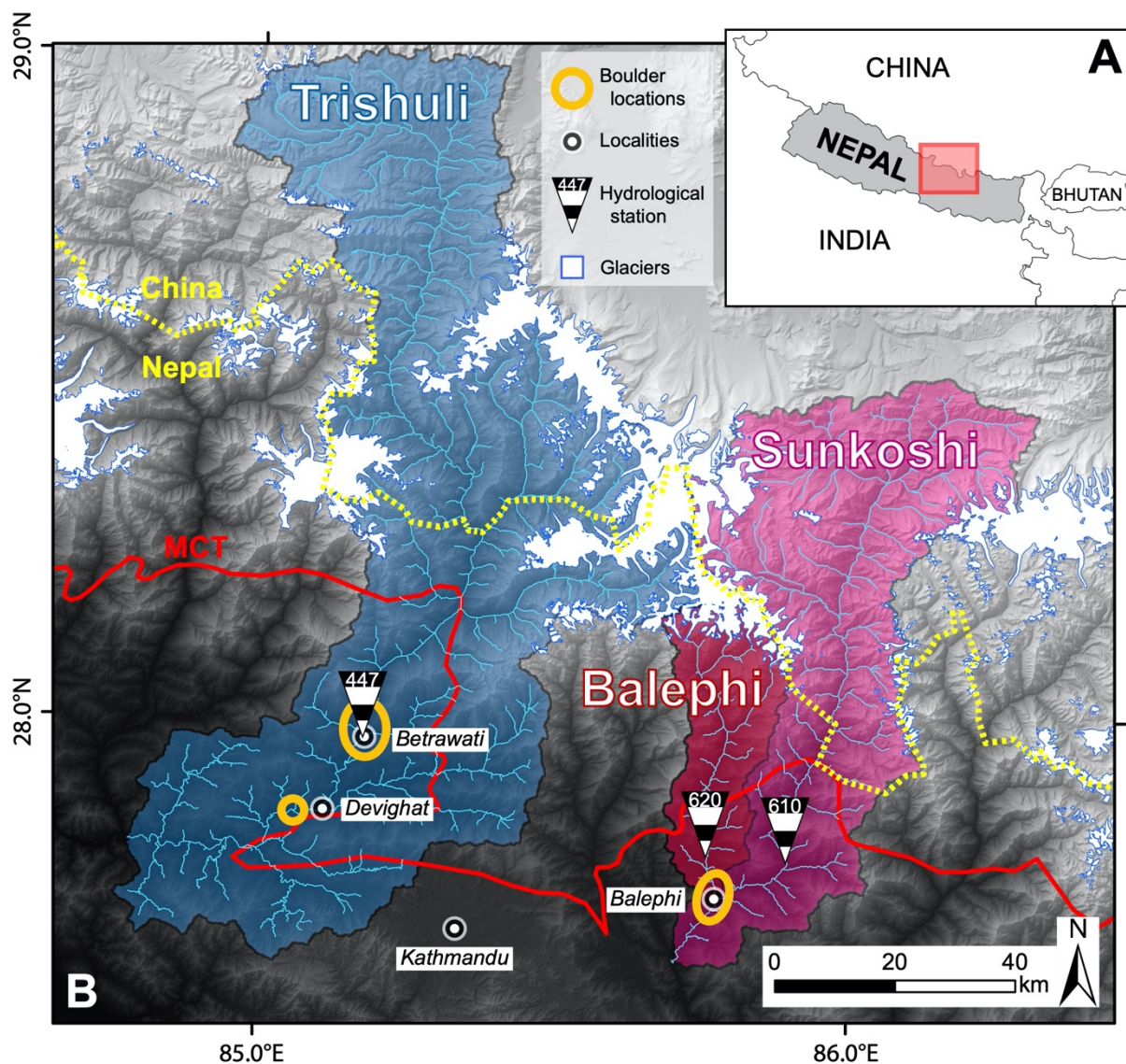
Richardson, S.D., Reynolds, J.M., 2000. An overview of glacial hazards in the Himalayas. Quaternary International 65, 31–
47.

Roback, K., Clark, M.K., West, A.J., Zekkos, D., Li, G., Gallen, S.F., Chamlagain, D., Godt, J.W., 2018. The size, distribution, and mobility of landslides caused by the 2015 Mw7. 8 Gorkha earthquake, Nepal. Geomorphology 301, 121–138.

Rosenwinkel, S., Landgraf, A., Schwanghart, W., Volkmer, F., Dzhumabaeva, A., Merchel, S., Rugel, G., Preusser, F., Korup, O., 2017. Late Pleistocene outburst floods from Issyk Kul, Kyrgyzstan? Earth Surf. Process. Landforms.

Ruiz-Villanueva, V., Allen, S., Arora, M., Goel, N.K., Stoffel, M., 2017. Recent catastrophic landslide lake outburst floods in the Himalayan mountain range. Progress in Physical Geography: Earth and Environment 41, 3–28.

Runqiu, H., 2009. Some catastrophic landslides since the twentieth century in the southwest of China. Landslides 6, 69–81.

Sapkota, S.N., Bollinger, L., Klinger, Y., Tapponnier, P., Gaudemer, Y., Tiwari, D., 2013a. Primary surface ruptures of the great Himalayan earthquakes in 1934 and 1255. Nature Geoscience 6, 71–76.

Sapkota, S.N., Bollinger, L., Klinger, Y., Tapponnier, P., Gaudemer, Y., Tiwari, D., 2013b. Primary surface ruptures of the great Himalayan earthquakes in 1934 and 1255. Nature Geoscience 6, 71.

Sarkar, S., Prasad, S., Wilkes, H., Riedel, N., Stebich, M., Basavaiah, N., Sachse, D., 2015. Monsoon source shifts during the drying mid-Holocene: Biomarker isotope based evidence from the core "monsoon zone"(CMZ) of India. Quaternary Science Reviews 123, 144–157.

Schaefer, J.M., Oberholzer, P., Zhao, Z., Ivy-Ochs, S., Wieler, R., Baur, H., Kubik, P.W., SchlUchter, C., 2008. Cosmogenic beryllium-10 and neon-21 dating of late Pleistocene glaciations in Nyalam, monsoonal Himalayas. Quaternary Science Reviews 27, 295–311.

Schwanghart, W., Worni, R., Huggel, C., Stoffel, M., Korup, O., 2016. Uncertainty in the Himalayan energy–water nexus: Estimating regional exposure to glacial lake outburst floods. Environmental Research Letters 11, 074005.

Schwanghart, W., Bernhardt, A., Stolle, A., Hoelzmann, P., Adhikari, B. R., Andermann, C., Tofelde, S., Merchel, S., Rugel, G., Fort, M. and Korup, O., 2016: Repeated catastrophic valley infill following medieval earthquakes in the Nepal Himalaya, Science, 351(6269), 147–150, doi:10.1126/science.aac9865.

Shang, Y., Yang, Z., Li, L., Liu, D., Liao, Q., Wang, Y., 2003. A super-large landslide in Tibet in 2000: background, occurrence, disaster, and origin. Geomorphology 54, 225–243.

Shrestha, AB, Eriksson, M., Mool, P., Ghimire, P., Mishra, B., Khanal, N.R., 2010. Glacial lake outburst flood risk assessment of Sun Koshi basin, Nepal. Geomatics, Natural Hazards and Risk 1, 157–169.

Shrestha, S.B., Shrestha, J.N., Sharma, S.R., 1986. Geological map of central Nepal.

Shroder, J.F., Cornwell, K., Khan, M.S., 1991. Catastrophic break-out floods in the western Himalaya, Pakistan, in:. Presented at the Geological Society of America Annual Meeting Program with Abstracts, p. A87.

Stoffel, M., Tiranti, D., Huggel, C., 2014. Climate change impacts on mass movements—case studies from the European Alps. Science of the Total Environment, The 493, 1255–1266.

Stolle, A., Bernhardt, A., Schwanghart, W., Hoelzmann, P., Adhikari, B.R., Fort, M., Korup, O., 2017. Catastrophic valley fills record large Himalayan earthquakes, Pokhara, Nepal. Quaternary Science Reviews 177, 88–103. doi:10.1016/j.quascirev.2017.10.015

620 Stolle, A., Schwanghart, W., Andermann, C., Bernhardt, A., Fort, M., Jansen, J.D., Wittmann, H., Merchel, S., Rugel, G., Adhikari, B.R., Korup, O., 2019. Protracted river response to medieval earthquakes. Earth Surf. Process. Landforms 44, 331–341. doi:10.1002/esp.4517

Stöcklin, J., 1980. Geology of Nepal and its regional frame: Thirty-third William Smith Lecture. Journal of the Geological Society 137, 1–34.

625 Thompson, L.O., Yao, T., Davis, M.E., Henderson, K.A., Mosley-Thompson, E., Lin, P.N., Beer, J., Synal, H.A., Cole-Dai, J., Bolzan, J.F., 1997. Tropical climate instability: The last glacial cycle from a Qinghai-Tibetan ice core. Science 276, 1821–1825.

Turowski, J.M., Yager, E.M., Badoux, A., Rickenmann, D., Molnar, P., 2009. The impact of exceptional events on erosion, bedload transport and channel stability in a step-pool channel. Earth Surf. Process. Landforms 34, 1661–1673.

630 Turzewski, M.D., Huntington, K.W., LeVeque, R.J., 2019. The geomorphic impact of outburst floods: Integrating observations and numerical simulations of the 2000 Yigong flood, eastern Himalaya. J. Geophys. Res. Earth Surf.

Upreti, B.N., 1999. An overview of the stratigraphy and tectonics of the Nepal Himalaya. Journal of Asian Earth Sciences 17, 577–606.

Veh, G., Korup, O., Specht, von, S., Roessner, S., Walz, A., 2019. Unchanged frequency of moraine-dammed glacial lake
635 outburst floods in the Himalaya. Nature Climate Change 9, 379.

Vuichard, D., Zimmermann, M., 1987. The 1985 catastrophic drainage of a moraine-dammed lake, Khumbu Himal, Nepal: cause and consequences. Mountain Research and Development 91–110.

Walder, J.S., Costa, J.E., 1996. Outburst floods from glacier-dammed lakes: the effect of mode of lake drainage on flood magnitude. Earth Surf. Process. Landforms 21, 701–723.

640 Wang, W., Xiang, Y., Gao, Y., Lu, A., Yao, T., 2015. Rapid expansion of glacial lakes caused by climate and glacier retreat in the Central Himalayas. Hydrol. Process. 29, 859–874.

Wang, Z.Y., Qi, P., Melching, C.S., 2009. Fluvial hydraulics of hyperconcentrated floods in Chinese rivers. Earth Surf. Process. Landforms 34, 981–993.

Wasson, R.J., Sundriyal, Y.P., Chaudhary, S., Jaiswal, M.K., Morthekai, P., Sati, S.P., Juyal, N., 2013. A 1000-year history of
645 large floods in the Upper Ganga catchment, central Himalaya, India. Quaternary Science Reviews 77, 156–166.

Willett, S.D., Brandon, M.T., 2002. On steady states in mountain belts. Geology 30, 175–178.

Wohl, E.E., 2013. Mountain rivers revisited: Ellen Wohl, Water resources monograph. Washington: American Geophysical Union. doi:10.1029/WM019

Worni, R., Stoffel, M., Huggel, C., Volz, C., Casteller, A., Luckman, B., 2012. Analysis and dynamic modeling of a moraine
650   failure and glacier lake outburst flood at Ventisquero Negro, Patagonian Andes (Argentina). Journal of Hydrology 444,
        134–145.

Xu, D., 1988. Characteristics of debris flow caused by outburst of glacial lake in Boqu river, Xizang, China, 1981. GeoJournal
        17, 569–580.

Yamada, T., Sharma, C.K., 1993. Glacier lakes and outburst floods in the Nepal Himalaya. IAHS Publications-Publications of
655   the International Association of Hydrological Sciences 218, 319–330.

Yamanaka, H., 1982. River terraces along the middle Kali Gandaki and Marsyandi Khola, central Nepal. J. Nepal Geol. Soc.
        2, 95–111.

Ziegler, A.D., Wasson, R.J., Bhardwaj, A., Sundriyal, Y.P., Sati, S.P., Juyal, N., Nautiyal, V., Srivastava, P., Gillen, J., Saklani,
        U., 2014. Pilgrims, progress, and the political economy of disaster preparedness–the example of the 2013 Uttarakhand
660   flood and Kedarnath disaster. Hydrol. Process. 28, 5985–5990.

Figure 1: A. Regional overview of the study area (red box). B. Location of the studied river reaches in central Nepal (main catchments of Trishuli and Sunkoshi, as well as Sunkhosi sub-catchment of Balephi), studied boulder locations and hydrological stations from the Nepal Department of Hydrology and Meteorology (along with station number). Also shown is the trace of the Main Frontal Thrust and glacier cover. Shaded relief is based on digital elevation model AW3D30, © Japan Aerospace Exploration Agency.
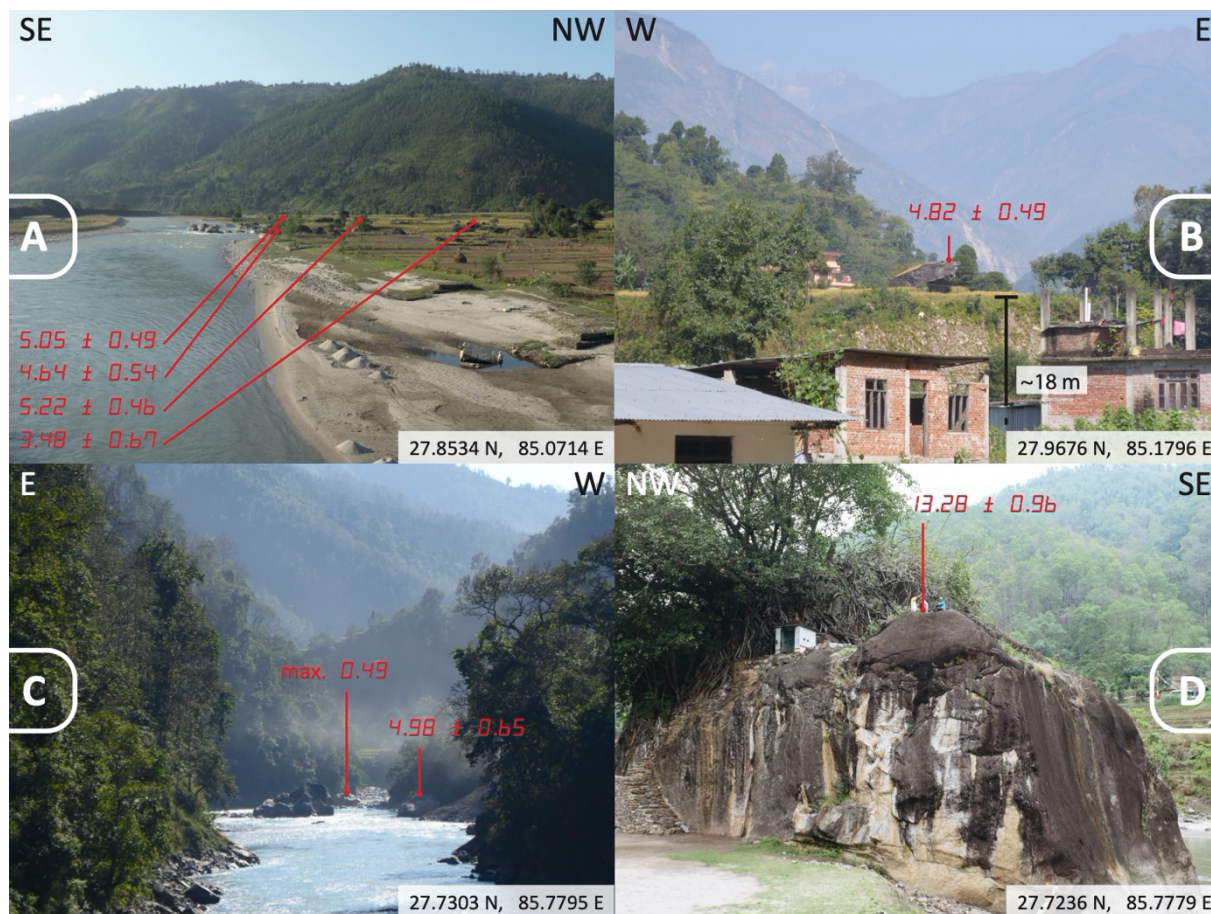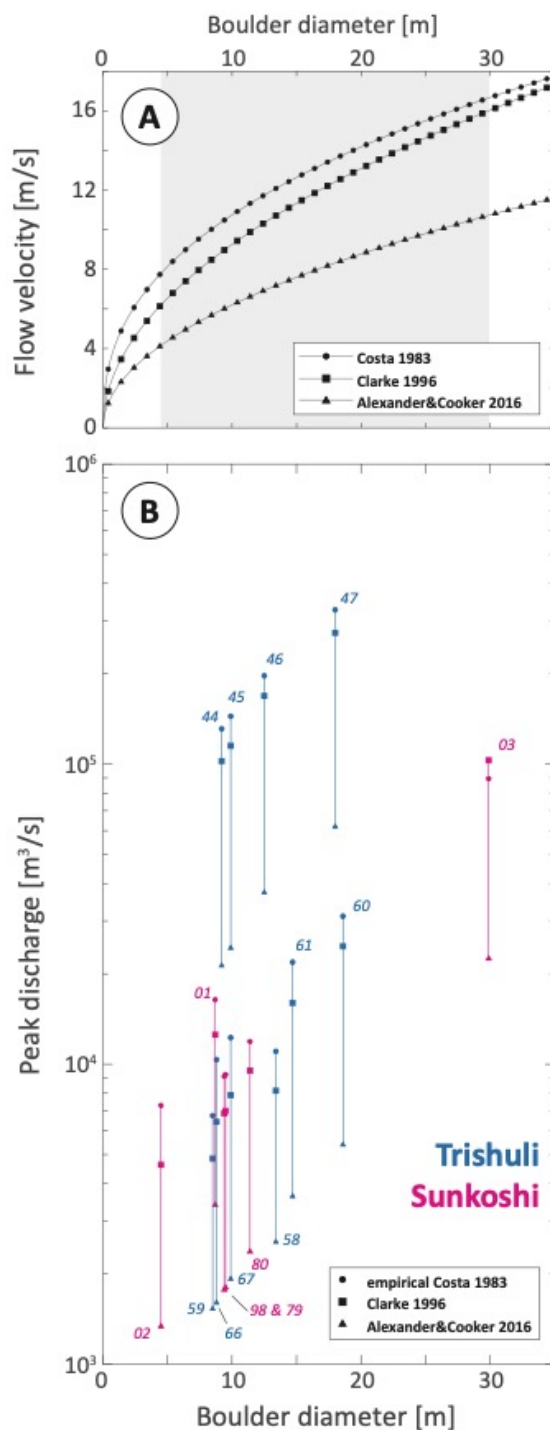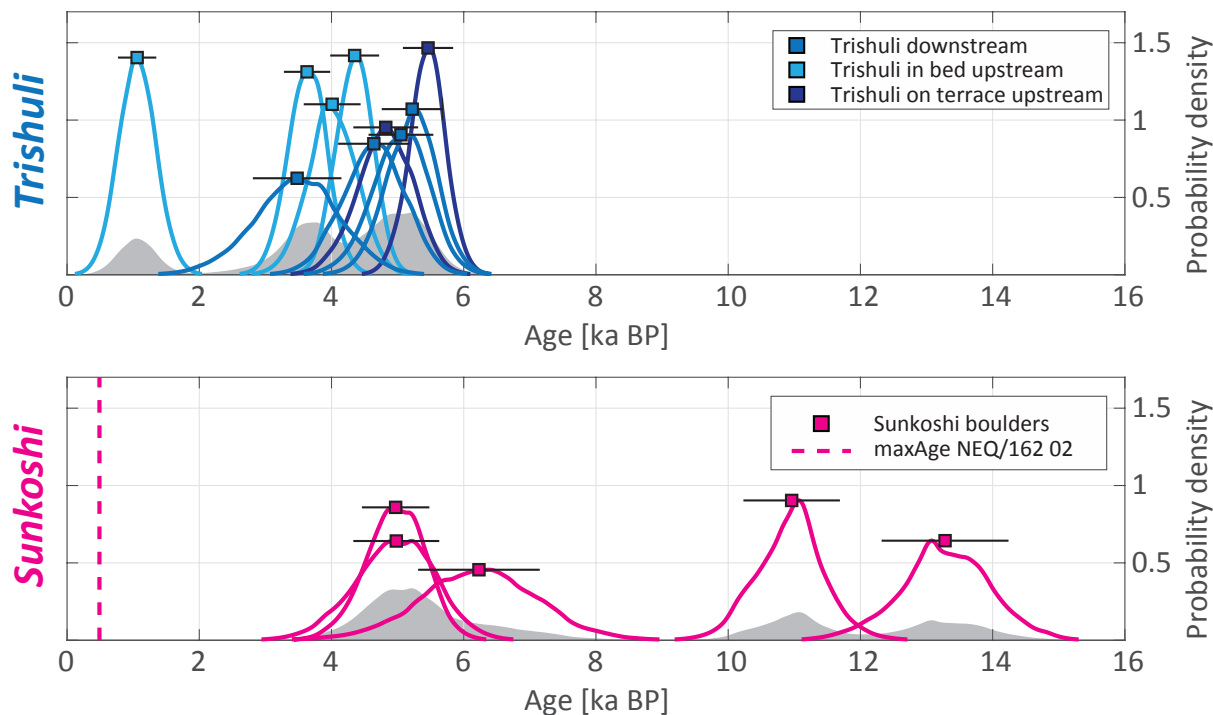
Figure 2: A- Boulders lying on a tributary fan south of Devighat, Trishuli valley. The main valley widens substantially at this location. Sample from top to bottom (as shown in the Figure): NEQ/162 47, ...46, ...45, ...44. B- Boulder appears sub-angular sitting on top of terrace deposit at Betrawatti (NEQ/162 66), Trishuli valley. In the background peaks rise >5000 m. C- Narrow part of Sunkoshi river after its confluence with Balephi Khola. Sample from top to bottom (as shown in the Figure): NEQ/161 02, ...01. D- Largest boulder surveyed in this study (NEQ/161 03) in Sunkoshi valley with an intermediate diameter of 29.9 m consists of gneiss lithology (Ulleri Gneiss), minimum travel distance 13 km. [10]Be surface exposure ages in ka BP. Coordinates of viewpoints given.
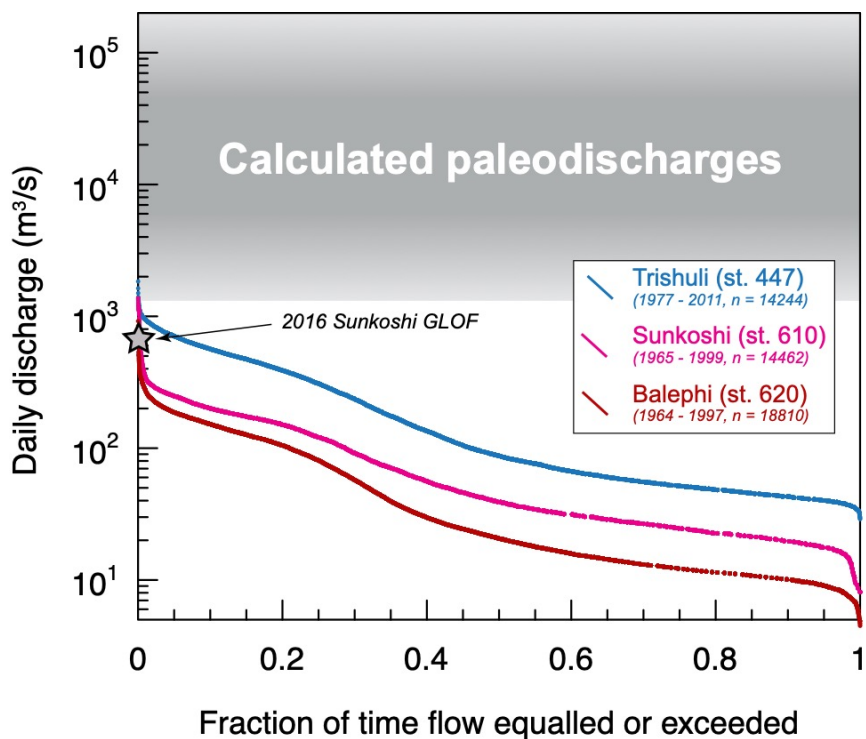
670

Figure 3: A- Theoretical flow velocities required to move boulders of a given diameter in an exemplary channel cross-section according to the parametrisations and models of Costa (1983), Clarke (1996) and Alexander and Cooker (2016). The grey shaded area indicates range of boulder intermediate diameters from this study. B- Estimated peak-paleo-discharges required to move the studied boulders according to the three models that were used for paleo-discharge calculations.
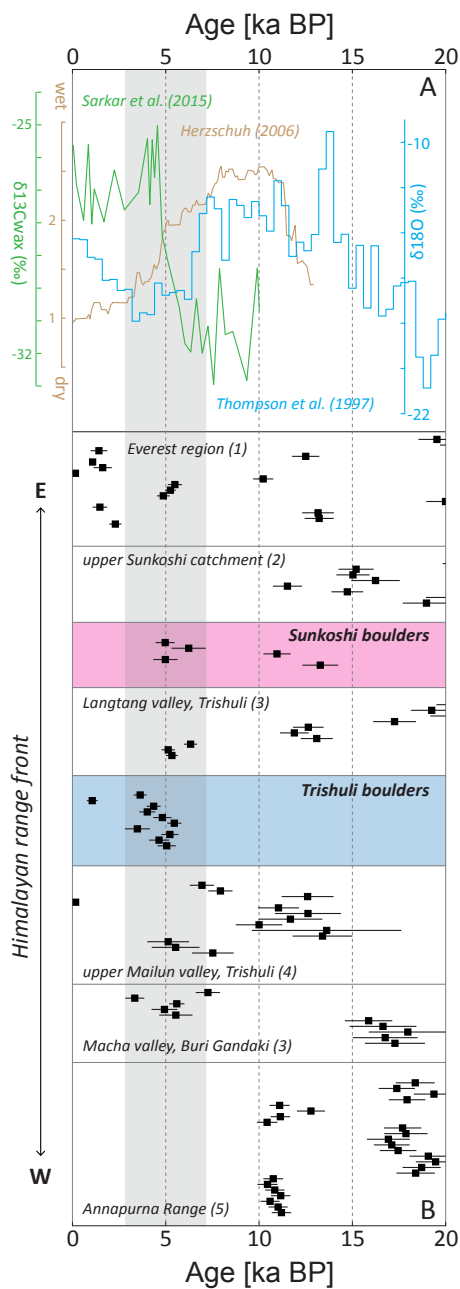
Figure 4: Probability density function for the [10]**Be boulder exposure ages in the Trishuli and Sunkoshi river reaches. The Trishuli boulders were subdivided in groups depending on boulder geographical location (upstream vs downstream) and position relative to the present-day channel. The grey shaded area in the background of each plot shows the cumulative sum of the probability distributions normalised by the quantity of boulders measured in the respective valley. Ages are indicated with 1σ error bars and were calculated using the online CREp calculator (Martin et al., 2017) accessed in June 2018 with a Sea Level High Latitude production rate of rate 4.08 ± 0.23 at/g/yr.**

Figure 5: Flow frequency curves of daily discharge data from the Trishuli at Betrawati (Station n# 447), the Sunkoshi in Barabise (Station n#610) and the Balephi Khola in Jalbire (Station n#620) along with the period covered by the data and the number of daily discharge measurements (Data from the Government of Nepal, Department of Hydrology and Meteorology). The range of paleo-discharges required to mobilise the studied boulders is shown in shades of grey. The discharge measured in Barabise for the 2016 GLOF on the Sunkoshi is also shown for comparison (Cook et al., 2018).

Figure 6: A- Climate proxy data: δ¹⁸O ice core measurements recovered on the Qinghai-Tibetan Plateau, China by Thompson et al. (1997); mean effective moisture index compiled from multiple paleoclimatic records in Indian monsoon dominated Asia by Herzschuh (2006); δ¹³Cwax (‰) vs VPDB lipid biomarker record from Lonar Lake central India by Sarkar et al. (2015). These proxies suggest a major climatic shift affecting monsoonal precipitation and consequently glacial dynamics on the south facing front at around 5 ka BP in the central Himalaya. **B-:** Boulder exposure ages in alignment with moraine deposits dated in the central Himalayan study region and recalculated consistently for better comparison: (1) Finkel et al. (2003), (2) Schaefer et al. (2008), (3) Abramowski et al. (2003), (4) Gayer et al. (2006), (5) Pratt-Sitaula et al. (2011). 1σ uncertainties are given with horizontal bars. Realm of boulder ages around 5 ka BP is accentuated with grey shading.

28

sample #	catchment	Lat [°]	Lon [°]	Alt. [m a.s.l.]	boulder intermediate diameter [m]	Lithology	Age(ka)	1σ (ka)	Minimum travel distance [km] (1)
NEQ/161 01	SUNKOSHI	27.72911	85.77910	674	8.7	orthogneiss	4.98	0.65	17
NEQ/161 02	SUNKOSHI	27.72805	85.77883	672	4.5	whitish orthogneiss	max. 0.49		17
NEQ/161 03	SUNKOSHI	27.72371	85.77810	668	29.9	ortho-, augengneiss, Ulleri Gneiss	13.28	0.96	13
NEQ/162 44	TRISHULI	27.85610	85.06961	441	9.2	orthogneiss	3.48	0.67	46 (13)
NEQ/162 45	TRISHULI	27.85601	85.06905	440	9.9	orthogneiss	5.22	0.46	46 (13)
NEQ/162 46	TRISHULI	27.85551	85.06886	445	12.5	orthogneiss	4.64	0.54	46 (13)
NEQ/162 47	TRISHULI	27.85589	85.06848	445	18	phyllitic schist	5.05	0.49	46 (13)
NEQ/162 58	TRISHULI	28.00898	85.18383	679	13.4	phyllite	3.63	0.35	0
NEQ/162 59	TRISHULI	28.00888	85.18438	680	8.5	orthogneiss	1.06	0.29	22
NEQ/162 60	TRISHULI	27.96964	85.18269	593	18.6	schist	4.35	0.37	0
NEQ/162 61	TRISHULI	27.96942	85.18208	593	14.7	schist	4.01	0.43	0
NEQ/162 66	TRISHULI	27.97021	85.17987	613	8.8	schist	4.82	0.49	0
NEQ/162 67	TRISHULI	27.97065	85.17986	613	9.9	phyllitic schist	5.46	0.38	0
NEQ/162 79	SUNKOSHI, Balephi	27.73503	85.78021	680	9.5	ortho-, augengneiss	6.23	0.92	16
NEQ/162 80	SUNKOSHI	27.73389	85.78328	695	11.4	ortho-, augengneiss	10.96	0.73	12
NEQ/162 98	SUNKOSHI, Balephi	27.74063	85.77722	693	9.4	ortho-, augengneiss	4.97	0.51	11

(1) in brackets if drainage from eastern, non-glaciated and smaller tributaries is included (i.e. shortest distance to MCT)

Table 1: Summary table of boulder location, lithology, minimum travel distance and exposure age. Further details can be found in the Supplement (S1 and S3).